

Rietveld Quantitative Analysis of *Buen Retiro* Porcelains

Antonio H. De Aza,^{†,‡} Ángeles G. De La Torre,[§] Miguel A. G. Aranda,[§] F. José Valle,[†] and Salvador De Aza^{**}

Instituto de Cerámica y Vidrio, Consejo Superiores de Investigaciones Científicas (CSIC)—Campus de Cantoblanco, Camino de Valdelatas s/n, 28049 Cantoblanco, Madrid, Spain

Departamento de Química Inorgánica, Cristalografía y Mineralogía, Universidad de Málaga, 29071 Málaga, Spain

Porcelains represent the foundation of the ceramic discipline. The variable-phase assembly within porcelains makes these materials very complex ceramics. Fine porcelains from *Buen Retiro* were produced between 1760 and 1808 by Spanish court ceramists. The factory and its records were totally destroyed in 1812 during the Peninsular War. Recently, some pieces of porcelain and remains of whiteware belonging to the ancient factory were discovered during an excavation. In the present work, some of the secret formulas that enabled the Spanish ceramists to produce porcelains have been investigated by quantitative full-phase analysis (including amorphous content) using the Rietveld method. Three porcelains belonging to the Sureda period (1803–1808) and another from an earlier time of the factory (1760–1783) have been analyzed. The phase results are discussed and conclusions are derived by using appropriate phase equilibrium diagrams. It has also been found that the Rietveld quantitative amorphous content analysis is effective in determining the glassy content in porcelains.

I. Introduction

THE arrival of Chinese porcelains (hard porcelains) in Europe in the eighteenth century involved a scientific, technological, and cultural breakthrough. These ceramic materials were so superior to any European product of the time that strenuous efforts were made to copy it. Fine porcelains of the *Buen Retiro* were produced from 1760 in jealously guarded secrecy in a factory in Madrid's Retiro Park. The factory was seized and turned into a fortified arsenal by Napoleon's occupying forces in 1808, then bombarded, sacked, and burnt to the ground by the Duke of Wellington's troops in 1812 during the Peninsular War. Its equipment and its records were totally destroyed. Recently 749 pieces and remains of whiteware belonging to the ancient factory were discovered during an excavation performed by the Dirección General de Patrimonio Cultural de la Comunidad Autónoma de Madrid at the place where the factory was located.¹

Madrid's local government has funded a research program that involves an interdisciplinary group of scientists to unravel the history and the secret formula that enabled Spanish court ceramists to produce porcelain. During this project,² it has been found that the porcelain belonging to the so-called Bartolomé Sureda period (1803–1808)^{3,4} is constituted by protoenstatite, α -quartz,

α -cristobalite, and vitreous phase. They used the locally available sepiolite from Vallecas^{2,5} for its manufacture. Sepiolite from Vallecas is considered, all over the world, as the standard sepiolite ($\text{Mg}_5[\text{Si}_8\text{O}_{20}][\text{OH}]_2[\text{H}_2\text{O}]_4 \cdot 4\text{H}_2\text{O}$).⁶ Bartolomé Sureda added part of this raw material previously calcined as a grog.^{2,5} The composition of the Sureda porcelain is different from any porcelain of the time. Additionally, some remains of whiteware with a different mineralogical composition have also been studied. One of these remains, belonging to an early age of the *Buen Retiro* factory (1760–1783),³ contains α -quartz, α -cristobalite, primary mullite, and vitreous phase, as was reported by De Aza *et al.*^{2,5}

However, these investigations did not provide information on the quantitative phase compositions of these porcelains. The goal of the present work is to perform a quantitative full-phase analysis (including the amorphous content) of fine porcelains of the *Buen Retiro* by Rietveld analysis. Three porcelains belonging to the Sureda period and another from an earlier age have been analyzed.

Rietveld methodology⁷ has had a very important impact on a broad scientific community as it is possible to address many problems concerning crystalline materials.⁸ A set of guidelines for the use of Rietveld refinement has been reported by the International Union of Crystallography Commission on powder diffraction.⁹ The Rietveld method was originally devised for the refinement of crystal and magnetic structures from powder neutron data, but nowadays it is also possible to determine quantitatively the amounts of crystalline phases even in complex samples.¹⁰ The Rietveld method is better suited for quantitative analysis (RQA) than other methods, such as reference intensity ratio (RIR) analysis, because it uses a wide diffraction range. The analysis of a wide pattern minimizes the inaccuracies arising from systematic errors within the raw data including peak overlap, preferred orientation, sample broadening, and lack of a pure standard. However, the crystal structures of all crystalline phases must be known to calculate the powder patterns. The outcome of the International Union of Crystallography Commission on powder diffraction round robin on quantitative phase analysis has been recently reported^{11,12} showing that RQA is the method that has the lowest errors. RQA is the subject of much research effort.^{13–15}

For many applications, it is also quite important to know the amorphous content within a given material. The quantification of amorphous phase(s) is a step forward in the use of RQA. Analyses of amorphous phases in crystalline samples by adding a suitable internal standard have very recently been reported.^{16–18}

The determination of the amorphous content in a given sample by RQA is straightforward. Initially, a mixture with a weighed amount of a suitable standard and the investigated material is prepared. The standard must have negligible, or at least a well-known, amorphous content. Then, the mixture is analyzed by powder diffraction with the Rietveld method. If the sample has amorphous phases, the crystalline phase(s) present in that sample will have a smaller Rietveld refined weight ratio(s) than that (those) calculated from the weight mixture. Therefore, the standard phase fraction will be overestimated. The procedure relates the amorphous phase content to the overestimation of the crystalline

W. E. Lee—contributing editor

Manuscript No. 10230. Received May 20, 2003; approved September 24, 2003. This work was financially supported by Project 06/0104/99: Dirección General de Investigación de la Consejería de Educación de la Comunidad de Madrid (2000–2001).

[†]CSIC—Campus de Cantoblanco.

[‡]To whom correspondence should be addressed. e-mail: aaza@icv.csic.es.

[§]Universidad de Málaga.

^{**}Fellow, American Ceramic Society.

standard in the Rietveld refinement. Such analyses can be applied to a single crystalline phase or to a multiphase sample.

Rietveld quantitative amorphous content analysis (RQACA) is nowadays a precise and accurate tool that allows the measurement of the amorphous phase content with accuracy close to 1 wt%. A protocol for such accurate analyses can be found elsewhere.¹⁷ However, it should be pointed out that the overall amorphous content determined by this method includes every minor crystalline phase not defined, all nondiffracting fractions such as vitreous phases, grain-boundary regions, and intrinsic defects, etc. So, the binding glassy fraction in a porcelain must be slightly lower than the overall amorphous content that can be determined from RQACA.

II. Experimental Procedure

(1) Specimen and Sample Preparations

Three remains of different whiteware belonging to the Bar-tolomé Sureda period (P8, P9, and P11) and another one (P510) of the early years of the *Buen Retiro* factory (1760–1783) have been analyzed. The selected samples were attributed to these two periods by specialists of the Spanish National Archaeological Museum (C. Mañueco and M. Granados),² taking into account different marks on the ceramic pieces.

The ceramic bodies of the porcelains were carefully separated from its glazes. First the pieces were machined by a 0.3-mm diamond saw. Next the specimens were rough-dressed with 320- μ m SiC sandpaper until all the glazes were removed. Then the samples were grounded to less than 35 μ m.

Standard α -Al₂O₃ was synthesized as follows: 6 g of γ -Al₂O₃ (99.997% from Alfa) was ground in a corundum ball-mill at 200 rpm for 30 min. Then, the powder was heated at 1100°C for 4 h in a Pt crucible. The oxide was cooled by turning off the furnace (to 150°C in \sim 5 h) and was ground at room temperature in a corundum mortar for 5 min. A second thermal treatment was conducted at 1200°C for 6 h and then cooled in the same way. The resulting standard was ground in a corundum mortar for 5 min and sieved (<35 μ m) before being weighed.

Each mixture was ground in a corundum mortar for 10 min, with acetone to help the particle dispersion, and then heated at 60°C. The mixtures with the standard were prepared to proportions of 29.683 wt% Al₂O₃/P8, 30.219 wt% Al₂O₃/P9, 32.461 wt% Al₂O₃/P11, and 30.763 wt% Al₂O₃/P510. The samples were gently loaded (vertically) into the aluminum X-ray sample holder.

(2) X-ray Data Collection

Laboratory X-ray powder diffraction (LXRPD) patterns were recorded on a Siemens D5000 automated diffractometer using CuK α _{1,2} radiations (1.5418 Å) and a secondary curved graphite monochromator. The data were collected in the Bragg–Brentano (θ /2 θ) vertical geometry (flat reflection mode) between 10° and 70° (2 θ) in 0.03° steps, counting for 25 s/step. The samples were rotated at 15 rpm during the acquisition to improve the powder averaging which is essential to have accurate intensities and, so, good phase analyses. The optic of the D5000 diffractometer was a system of primary Soller foils between the X-ray tube and the fixed aperture slit of 2 mm. One scattered-radiation slit of 2 mm was placed after the sample, followed by a system of secondary Soller slits and the detector slit of 0.2 mm. The X-ray tube operated at 40 kV and 30 mA.

(3) X-ray Data Analysis

The powder patterns were refined by the Rietveld method with the GSAS suite of programs¹⁹ by using a pseudo-Voigt peak shape function²⁰ with the asymmetry correction of Finger *et al.*²¹ included. When preferred orientation was observed in the patterns, it was corrected via the March–Dollase algorithm²² (e.g., protoenstatite along the [010] direction). The crystal structures used to calculate the powder patterns are given in Table I. The absorption coefficients for CuK α _{1,2} are also listed. The anisotropic vibration temperature factors were converted to corresponding isotropic values. The positional and thermal vibration parameters were not refined. The optimized parameters were: background coefficients, cell parameters, zero-shift error, peak shape parameters (including anisotropic terms if needed), preferred orientation (when appropriate), and phase fractions.

(4) Chemical Analysis

The ceramic bodies of the porcelains (without its glazes) were analyzed by using X-ray fluorescence (XRF) and flame emission spectrometry (FES). The XRF analyses were performed using a Philips PW-1404 XRF spectrometer. This device is a Sc/month dual-anode instrument. Additionally, a 2100 Perkin-Elmer atomic absorption spectrometer was used in flame emission spectrophotometer mode to perform the FES. Alkaline analyses (Na and K) were conducted by measuring emission lines at 589 and 766 nm, respectively. The flame effect (air/acetylene) on the ionization of both elements was minimized by adding NH⁺ to samples and standards. The chemical analyses of the studied porcelains are listed in Table II.

III. Results

As mentioned previously, RQACA relates the overall amorphous content, *A* (wt%), to the overestimation of an internal crystalline standard in the Rietveld refinement. Considering a standard free of amorphous phases, *A* is obtained from the following equation:

$$A = \frac{1 - (W_s/R_s)}{100 - W_s} \times 10^4 \quad (1)$$

where *W_s* (%) is the weighed concentration of the internal standard and *R_s* (wt%) is the Rietveld analyzed concentration of the internal standard.

The Rietveld plots (15–70°/2 θ) for the four analyzed samples are shown in Figs. 1(a) to (d). The values of the pattern-dependent, *R_{WP}* disagreement factor^{7,8,19} were evaluated, and they are listed in Table III. The values are smaller than 10%, indicating good fits; see also the flatness of the difference curves in Fig. 1. Furthermore, the values of the phase-dependent, *R_p*, disagreement factor^{7,8,19} are quite small; see Table III, which indicates that fits to any given phase are very satisfactory.

The final phase compositions for the four porcelains from the full RQA are given in Table IV. The overall amorphous phase contents of the analyzed porcelains were derived from the refined Al₂O₃ phase ratios, Table III, by using Eq. (1). The phase fractions of the crystalline components obtained directly in the Rietveld study have to be renormalized by taking into account the overall nondiffracting fraction.

Table I. Some Structural Details of the Investigated Phases

| Mineral name | Chemical formula | Absorption coefficient [†] | PDF file number | ICSD collection code | Reference |
|------------------------|--|-------------------------------------|-----------------|----------------------|------------------------------------|
| Corundum | Al ₂ O ₃ | 121.4 | 43-1484 | 73 725 | Maslen <i>et al.</i> ³³ |
| Mullite | 3Al ₂ O ₃ ·2SiO ₂ | 99.44 | 15-776 | 66 263 | Angel <i>et al.</i> ³⁴ |
| Protoenstatite | MgO·SiO ₂ | 97.12 | 11-0273 | 36 262 | Smith ³⁵ |
| α -Quartz | SiO ₂ | 89.53 [‡] | 46-1045 | 63 532 | Will <i>et al.</i> ³⁶ |
| α -Cristobalite | SiO ₂ | 78.46 [‡] | 39-1425 | 34 928 | Peacor ³⁷ |

[†]Linear absorption coefficient, μ , in cm⁻¹. [‡]The difference in μ is due to their different densities.

Table II. Chemical Analyses of the Studied Porcelains

| Species | Buen Retiro porcelains | | | | Analytical method |
|--------------------------------|------------------------|----------|-----------|------------|-------------------|
| | P8 (wt%) | P9 (wt%) | P11 (wt%) | P510 (wt%) | |
| SiO ₂ | 77.3 | 77.7 | 76.9 | 76.2 | XRF |
| Al ₂ O ₃ | 8.76 | 8.68 | 10.1 | 18.8 | XRF |
| Fe ₂ O ₃ | 0.089 | 0.076 | 0.074 | 0.49 | XRF |
| CaO | 0.14 | 0.88 | 0.85 | 0.070 | XRF |
| TiO ₂ | 0.002 | 0.010 | 0.001 | 0.007 | XRF |
| MnO | 0.030 | 0.003 | 0.010 | 0.012 | XRF |
| MgO | 10.6 | 8.91 | 9.23 | 0.79 | XRF |
| P ₂ O ₅ | 0.22 | 0.17 | 0.19 | 0.16 | XRF |
| K ₂ O | 1.54 | 1.11 | 0.93 | 1.20 | FES |
| Na ₂ O | 0.58 | 0.85 | 0.90 | 0.55 | FES |
| Total | 99.2 | 98.4 | 99.1 | 98.3 | — |

IV. Discussion

To determine the amorphous phase content of a crystalline sample by RQACA, a standard with a negligible (or at least well-determined) amorphous content is needed. Additionally, it must be kept in mind that the overall amorphous content determined via RQACA may come from several sources, as was discussed in the Introduction.

Al₂O₃ with the corundum structure was found to be the best standard for the case study. This compound was overestimated in all previous refinements, indicating that it has a negligible amorphous content.¹⁷ So, we assume in this study that the Al₂O₃ standard is free from amorphous phases. Additionally, Al₂O₃ displays little preferred orientation, which dramatically increases the errors of the analyses; it has small (lower than 1 μ m) grain size,

which helps to obtain accurate intensities as enough particles diffract in any direction; and the peak shape is easy to model.

For accurate phase analysis, microabsorption has to be taken into account. A method to partially correct this effect was developed by Brindley²³ and related to the Rietveld methodology by Taylor.²⁴ A detailed description of this correction has recently been presented.²⁵ To minimize the microabsorption-associated errors, the standard and the sample phases must have similar values of the absorption coefficients. As can be seen in Table I, Al₂O₃ is a suitable standard as its absorption coefficient is very similar to those of the phases in these porcelains. In the present case, the absorption coefficients of all phases are very similar; see Table I. Hence, microabsorption effect is not a problem, and its correction is not needed.

It should be noted that the reported standard deviations for the amorphous content and the crystalline phases are those directly derived from the Rietveld least-squares analysis. These values are slightly underestimated because they only take into account the statistic of the intensities in the pattern. The systematic errors usually found in a powder diffraction experiment which are not accounted in the error analysis of the Rietveld method are as follows: no perfect powder averaging for all phases in the holder, inadequate peak shape descriptions in the fits, and small differences between the used crystal structure and those of the phase in the mixtures, etc.

The results of the RQACA of P510 porcelain (Table IV) showed that it is constituted by 41.9 wt% α -quartz, 1.8 wt% α -cristobalite, 21.7 wt% mullite, and 34.6 wt% glassy phase.

Additionally, from the chemical analyses, as can be seen in Table II, the main components of this porcelain are SiO₂ (76.2 wt%), Al₂O₃ (18.8 wt%), and alkalis (K₂O + Na₂O) (1.75 wt%).

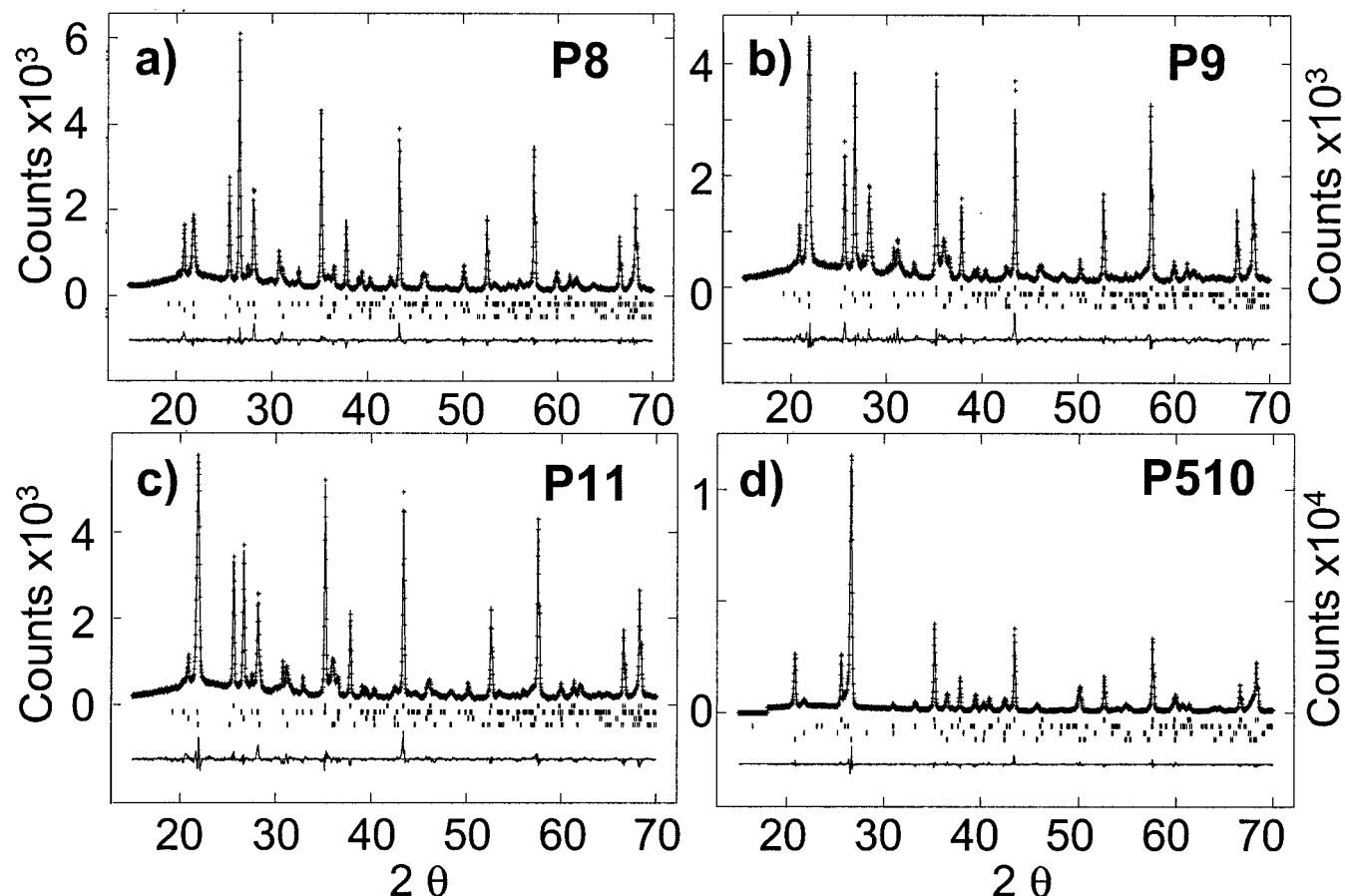


Fig. 1. (a) to (d) RQACA Rietveld plots (15–70°/2 θ) for the four analyzed samples with the observed (crosses), calculated (line), and difference (bottom line) powder patterns. The marks correspond to the Bragg peaks of the different phases. (a) to (c), from bottom to top: α -cristobalite, α -quartz, protoenstatite, and corundum (standard). Panel d: α -quartz, α -cristobalite, mullite, and corundum (standard).

Table III. Some Rietveld Refinement Results for the Porcelains Mixed with Al_2O_3 [†]

| Sample | $W_S(\text{Al}_2\text{O}_3)$ (%) | $R_S(\text{Al}_2\text{O}_3)$ (%) | R_{WP} (%) | $R_F(\text{Al}_2\text{O}_3)$ (%) | $R_F(\text{Q})$ (%) | $R_F(\alpha\text{-S})$ (%) | $R_F(\text{MS or A}_3\text{S}_2)$ (%) |
|--------|----------------------------------|----------------------------------|--------------|----------------------------------|---------------------|----------------------------|---------------------------------------|
| P8 | 29.68 | 50.0(2) | 7.73 | 2.06 | 2.56 | 4.35 | MS 4.72 |
| P9 | 30.22 | 49.1(2) | 8.57 | 2.92 | 3.09 | 2.83 | MS 5.12 |
| P11 | 32.46 | 52.0(2) | 7.95 | 2.53 | 3.91 | 2.68 | MS 4.97 |
| P510 | 30.76 | 40.5(3) | 7.57 | 1.93 | 1.67 | 2.96 | A_3S_2 2.67 |

[†]Cement notation is used in the tables, i.e. A is Al_2O_3 , M is MgO, and S is SiO_2 . Therefore, A_3S_2 stands for mullite, MS stands for protoenstatite, $\alpha\text{-S}$ stands for α -cristobalite, and Q stands for α -quartz.

The rest of the chemical species are minus impurities that must be in the glassy phase. Thus, the composition, expressed as a function of the three mentioned main oxides, can be represented within the $\text{SiO}_2\text{--Al}_2\text{O}_3\text{--K}_2\text{O}$ ternary system,²⁶ point that has been denoted as P_{510} in Fig. 2.

On the other hand, keeping in mind the percentage of the diverse crystalline phases, determined by RQACA (Table IV), and subtracting the percentages of the corresponding oxides (15.6 wt% Al_2O_3 and 49.8 wt% SiO_2) from the chemical analysis (Table II), the composition of the vitreous phase can be determined in the function of the main oxides: 84.2 wt% SiO_2 , 10.2 wt% Al_2O_3 , and 5.6 wt% alkalis ($\text{K}_2\text{O} + \text{Na}_2\text{O}$). The residual weight percents of the minus impurities determined by chemical analysis are considered negligible. Consequently, the composition location of this amorphous phase is shown in Fig. 2 by the point denoted as L_{510} . As can be observed, the composition of the liquid phase lays very close to the binary eutectic line that separates the primary phase fields of mullite and silica. From its location, it can be estimated that the firing temperature of the porcelain was $\sim 1400^\circ\text{C}$, which agrees with that indicated by De Aza et al.^{2,5}

Further, the proportions of crystalline SiO_2 (α -quartz + α -cristobalite) and $3\text{Al}_2\text{O}_3\cdot 2\text{SiO}_2$ are known (66.8 and 33.2 wt%, respectively), which represents 65.4% of the whole porcelain composition (Table IV). As mentioned above, the remainder up to 100% is constituted by all nondiffracting fractions such as vitreous phases, grain-boundary regions, and intrinsic defects, etc. This overall amorphous content represents the 34.6 wt% of the composition that here is considered as glassy phase. Thus, the composition of the porcelain derived from the RQACA can be located within the mentioned ternary system by applying the lever rule.²⁷ This point has been denoted as R_{510} in Fig. 2.

As can be seen, data derived from the chemical analysis and the Rietveld method are in close agreement.

Consequently the studied composition is located inside the primary phase field of the crystallization of mullite within the subsystem $\text{SiO}_2\text{--K}_2\text{O}\cdot\text{Al}_2\text{O}_3\cdot 6\text{SiO}_2\text{--}3\text{Al}_2\text{O}_3\cdot 2\text{SiO}_2$, where the so-called hard porcelains are located. These are normally obtained from different proportions of quartz, feldspar, and kaolin.²⁸ However, according to De Aza et al.,^{2,5} the porcelain studied has been manufactured without any feldspar addition using a clay called Garlitos,²⁹ which is a mixture of kaolinite and sericite. It seems that the sample has been formulated as Song dynasty Chinese porcelains (960–1280).³⁰

On the other hand, the results of the three quantitative Rietveld analyses for P8, P9, and P11 porcelains (Table IV) showed that these porcelains are constituted by different amounts of α -quartz, α -cristobalite, protoenstatite, and a glassy phase. The chemical compositions of these porcelains have around 1–2 wt% alkalis

($\text{K}_2\text{O} + \text{Na}_2\text{O}$) and other minus impurities in the glass (Table II). Keeping in mind their main constituents SiO_2 , Al_2O_3 , MgO, and $\text{K}_2\text{O} + \text{Na}_2\text{O}$, their compositions have been located inside the system $\text{SiO}_2\text{--MgSiO}_4\text{--K}_2\text{O}\cdot\text{Al}_2\text{O}_3\cdot 4\text{SiO}_2$ ^{31,32} (Fig. 3), represented by the letters P_8 , P_9 , and P_{11} , respectively.

Proceeding as in the previous case, the composition of the liquid phases as a function of the main oxides, in the three porcelains, has been calculated. The results of these calculations are graphically shown in Fig. 3 by the points denoted as L_8 , L_9 , and L_{11} , respectively. Similarly, in Fig. 3, the composition of the three porcelains derived from the RQACA, considering the percentages of protoenstatite, silica (α -quartz + α -cristobalite), and liquid phase, has been located within the $\text{SiO}_2\text{--MgSiO}_4\text{--K}_2\text{O}\cdot\text{Al}_2\text{O}_3\cdot 4\text{SiO}_2$ ternary system by applying the above-mentioned lever rule. These points have been denoted as R_8 , R_9 , and R_{11} , respectively. As can be appreciated, the data derived from chemical analyses and the Rietveld method also agree well in these porcelains.

The compositions of these porcelains are located within the primary phase field of crystallization of protoenstatite inside the subsystem $\text{SiO}_2\text{--K}_2\text{O}\cdot\text{Al}_2\text{O}_3\cdot 6\text{SiO}_2\text{--MgO}\cdot\text{SiO}_2$. Consequently, during the firing process, the first formation of the liquid phase takes place at 985°C , the invariant point of the subsystem. As the temperature rises from 985° to $\sim 1400^\circ\text{C}$, the estimated firing temperature of the porcelain,^{2,4,5} the amount of liquid slightly increases. Despite the rising temperature, its viscosity remains practically constant due to the growing content in silica since the

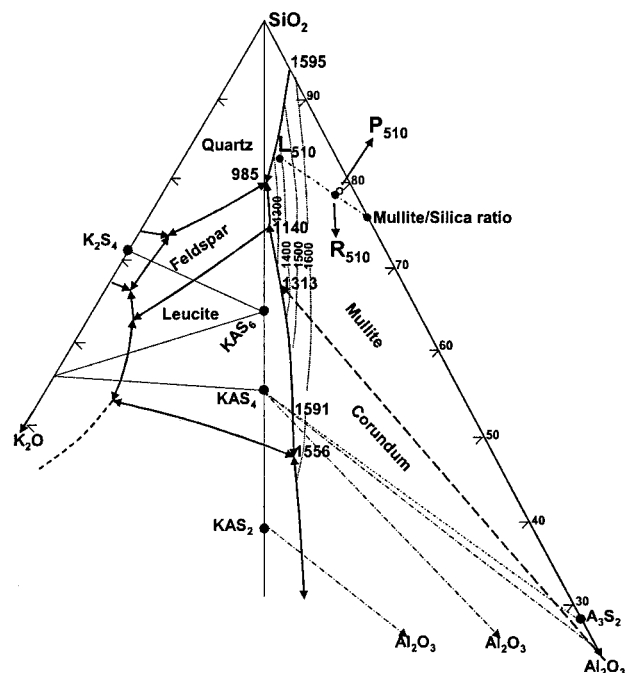


Fig. 2. Detail of $\text{SiO}_2\text{--Al}_2\text{O}_3\text{--K}_2\text{O}$ ternary system.²⁶ The composition of P_{510} porcelain is located within the compatibility triangle $\text{SiO}_2\text{--K}_2\text{O}\cdot\text{Al}_2\text{O}_3\cdot 6\text{SiO}_2\text{--}3\text{Al}_2\text{O}_3\cdot 2\text{SiO}_2$. P_{510} and R_{510} stand for the composition of the porcelain derived from chemical analysis and Rietveld analysis, respectively. L denotes the vitreous phase composition.

Table IV. Phase Composition of the Porcelains from Full Quantitative Rietveld Analysis[†]

| Sample | α -Quartz (%) | α -Cristobalite (%) | Protoenstatite or mullite (%) | Amorphous (%) |
|--------|----------------------|----------------------------|--------------------------------|---------------|
| P8 | 15.5(2) | 6.4(2) | MS 20.2(3) | 57.9(5) |
| P9 | 10.9(2) | 19.8(3) | MS 14.2(4) | 55.1(6) |
| P11 | 7.9(2) | 21.5(3) | MS 15.0(3) | 55.6(4) |
| P510 | 41.9(7) | 1.8(1) | A_3S_2 21.7(5) | 34.6(5) |

[†]See Table III for notation used.

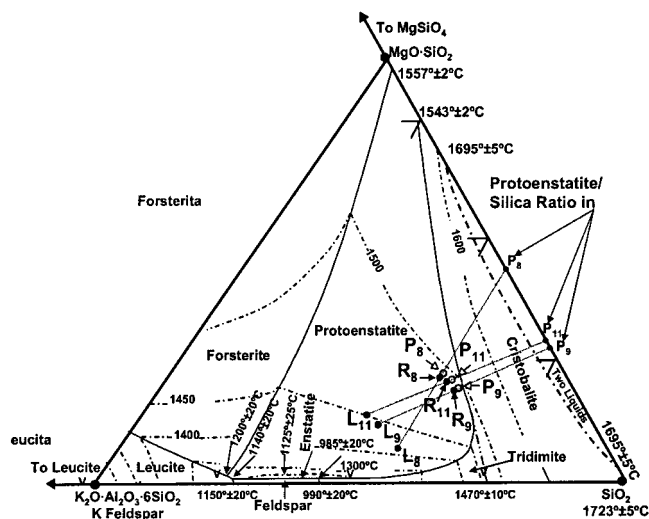


Fig. 3. $\text{SiO}_2\text{-MgSiO}_4\text{-K}_2\text{O-Al}_2\text{O}_3\text{-4SiO}_2$ ternary system.^{31,32} The compositions of P8, P9, and P11 porcelains are located within the subsystem: $\text{SiO}_2\text{-K}_2\text{O-Al}_2\text{O}_3\text{-6SiO}_2\text{-MgO-SiO}_2$. P8, P9, P11 and R8, R9, and R11 stand for the compositions of the porcelain derived from chemical analyses and Rietveld analyses, respectively. L8, L9, and L11 denote the vitreous phase compositions.

binary eutectic line that separates the protoenstatite and silica primary fields goes practically parallel to the edge $\text{SiO}_2\text{-K}_2\text{O-Al}_2\text{O}_3\text{-4SiO}_2$. This avoids the material deformation during the firing process and justifies the wide firing range of these materials. In equilibrium conditions, the Sureda porcelain should be constituted by protoenstatite, α -cristobalite, and a vitreous phase. The coexistence of α -quartz means nonequilibrium conditions and the location of the glassy phases away from the boundary line also. Likewise, the dispersion of phase ratios found in this study has to be due either to fluctuations in firing temperature or in composition.

All that exposed justifies the differences found in the percentages of the mineralogical compositions of the studied samples as well as the easiness of manufacturing (due to the wide firing range) of the compositions used by Bartolomé Sureda.

V. Conclusions

The following concluding remarks can be made:

(a) The three analyzed porcelains belonging to the Bartolomé Sureda period (1803–1808) are composed of the following range of phases: protoenstatite (14–20 wt%), α -quartz (8–15 wt%), α -cristobalite (6–21 wt%), and amorphous phase(s) (55–58 wt%).

(b) Fluctuations in soaking temperature or in raw material compositions would give rise to the dispersion of phase ratios found in this set of porcelains.

(c) The analyzed porcelain belonging to an early age of the Buen Retiro factory (1760–1783) is composed of α -quartz (42 wt%), α -cristobalite (2 wt%), mullite (22 wt%), and amorphous phase (34 wt%).

(d) Last but not least, quantitative full-phase analysis (including the amorphous content) by the Rietveld method using laboratory X-ray powder diffraction is a suitable technique to characterize the mineralogical composition of porcelains.

Acknowledgments

The authors acknowledge the contribution of Dr. Pilar Pena in offering valuable suggestions and stimulating discussion during the course of this work.

References

- ¹F. Marín, P. Mena, A. Vigil-Escalera, G. Yañez-Santiago, A. Kermovant, and J. L. Lorenzo, "La intervención arqueológica en el Parque del Retiro (El Huerto del

Francés)" (Archaeological research at the Retiro Park: The French's Orchard); pp. 129–44 in *Manufactura del Buen Retiro 1760–1808*. Catálogo de la Exposición de Porcelanas del Buen Retiro, Museo Arqueológico Nacional, Madrid, Spain, 1999.

²S. De Aza, E. Criado, R. Martínez, F. J. Valle, J. M. Fernández Navarro, J. M. Rincón, M. S. Hernández, M. Regueiro, L. Céspedes, M. Becerril, A. López Alonso, L. Cuarta, P. Mena, F. J. Marín, G. Yañez, S. Quero, C. Mañueco, and M. Granados, Las Cerámicas del Buen Retiro (Buen Retiro Porcelains) Project 06/0104/99. Supported by the Dirección General de Investigación de la Consejería de Educación de la Comunidad de Madrid. (2000–2001). CD-Rom edited by S. De Aza (aza@icv.csic.es), 2002.

³M. Pérez-Villamil, "El laboratorio de piedras duras y mosaico obradores de bronce y marfiles"; p. 50 in *Artes e industrias de Buen Retiro. La Fábrica de la China* (Arts and Industries of Buen Retiro. The Chinese Factory). Edited by Est. Tip. Sucesores de Rivadeneyra. Impresores de la Real Casa, Madrid, Spain, 1904.

⁴C. Mañueco, M. Granados, S. Quero, P. Mena, F. J. Marín, G. Yañez, M. Becerril, A. López Alonso, L. Cuarta, M. Regueiro, L. Céspedes, J. M. Rincón, M. S. Hernández, S. De Aza, E. Criado, R. Martínez, F. J. Valle, and J. M. Fernández Navarro, "Las porcelanas de Buen Retiro" (Buen Retiro Porcelains), *Bol. Soc. Esp. Ceram. Vidrio*, **40** [3] 1–10 (2001).

⁵S. De Aza, F. J. Valle, E. Criado, and R. Martínez, "La fábrica de porcelanas del Buen Retiro. La época de Bartolomé Sureda" (The Porcelains Factory of Buen Retiro. The Bartolomé Sureda Period), VII Congreso Nacional de Materiales, Madrid, Spain, October 16–18, 2002.

⁶E. Galán Huertos, "Palygorskita y Sepiolita"; pp. 71–94 in *Recursos Minerales de España*. Edited by J. García Guinea and J. Martínez Frías, Textos Universitarios. Consejo Superior de Investigaciones Científicas, 1992.

⁷H. M. Rietveld, "A Profile Refinement Method for Nuclear and Magnetic Structures," *J. Appl. Crystallogr.*, **2**, 65–71 (1969).

⁸R. A. Young, *The Rietveld Method*. Oxford University Press, Oxford, U.K., 1993.

⁹L. B. McCusker, R. B. Von Dreele, D. E. Cox, D. Louer, and P. Scardi, "Rietveld Refinements Guidelines," *J. Appl. Crystallogr.*, **32**, 36–50 (1999).

¹⁰R. J. Hill and C. J. Howard, "Quantitative Phase Analysis from Neutron Powder Diffraction Data Using the Rietveld Method," *J. Appl. Crystallogr.*, **20**, 467–74 (1987).

¹¹I. C. Madsen, N. V. Y. Scarlett, L. M. D. Cranswick, and T. Lwin, "Outcomes of the International Union of Crystallography Commission on Powder Diffraction Round Robin on Quantitative Phase Analysis: Samples 1a to 1h," *J. Appl. Crystallogr.*, **34**, 409–26 (2001).

¹²N. V. Y. Scarlett, I. C. Madsen, L. M. D. Cranswick, T. Lwin, E. Groleau, G. Stephenson, M. Aylmore, and N. Agron-Olshina, "Outcomes of the International Union of Crystallography Commission on Powder Diffraction Round Robin on Quantitative Phase Analysis: Samples 2, 3, 4, Synthetic Bauxite, Natural Granodiorite and Pharmaceuticals," *J. Appl. Crystallogr.*, **35**, 383–400 (2002).

¹³H. Toraya, "Quantitative Phase Analysis of α - and β -Silicon Nitrides. I. Estimation of Errors," *J. Appl. Crystallogr.*, **32**, 704–15 (1999).

¹⁴H. Toraya, "Estimation of Statistical Uncertainties in Quantitative Phase Analysis Using the Rietveld Method and the Whole-Powder-Pattern Decomposition Method," *J. Appl. Crystallogr.*, **33**, 1324–28 (2000).

¹⁵A. G. De La Torre, A. Cabeza, A. Calvente, S. Bruque, and M. A. G. Aranda, "Full Phase Analysis of Portland Clinker by Penetrating Synchrotron Powder Diffraction," *Anal. Chem.*, **73**, 151–56 (2001).

¹⁶R. S. Winburn, D. G. Grier, G. J. McCarthy, and R. B. Peterson, "Rietveld Quantitative X-ray Diffraction Analysis of NIST Fly Ash Standard Reference Materials," *Powder Diffr.*, **15**, 163–72 (2000).

¹⁷A. G. De La Torre, S. Bruque, and M. A. G. Aranda, "Rietveld Quantitative Amorphous Content," *J. Appl. Crystallogr.*, **34**, 196–202 (2001).

¹⁸P. M. Suherman, A. van Riessen, B. O'Connor, D. Bolton, and H. Fairhurst, "Determination of Amorphous Phase Levels in Portland Cement Clinker," *Powder Diffr.*, **17**, 178–85 (2002).

¹⁹A. C. Larson and R. B. Von Dreele, Los Alamos National Laboratory Report No. LA-UR-86-748. Los Alamos National Laboratory, Los Alamos, NM, 1994. GSAS program at <http://public.lanl.gov:80/gsas/>.

²⁰P. Thompson, D. E. Cox, and J. B. Hastings, "Rietveld Refinement of Debye-Scherrer Synchrotron X-ray Data from Al_2O_3 ," *J. Appl. Crystallogr.*, **20**, 79–83 (1987).

²¹L. W. Finger, D. E. Cox, and A. P. Jephcoat, "A Correction for Powder Diffraction Peak Asymmetry Due to Axial Divergence," *J. Appl. Crystallogr.*, **27**, 892–900 (1994).

²²W. A. Dollase, "Correction of Intensities for Preferred Orientation in Powder Diffraction: Application of the March Model," *J. Appl. Crystallogr.*, **19**, 267–72 (1986).

²³G. W. Brindley, "The Effect of Grain or Particle Size on X-ray Reflection from Mixed Powders and Alloys, Considered in Relation to the Quantitative Determination of Crystalline Substances by X-ray Methods," *Philos. Mag.*, **36**, 347–69 (1945).

²⁴J. C. Taylor, "Computer Programs for Standardless Quantitative Analysis of Minerals Using the Full Powder Diffraction Profile," *Powder Diffr.*, **6**, 2–9 (1991).

²⁵R. S. Winburn, S. L. Lerach, B. R. Jarabek, M. A. Wisdom, D. G. Grier, and G. McCarthy, "Quantitative XRD Analysis of Coal Combustion By-products by the Rietveld Method. Testing with Standard Mixtures"; pp 387–96 in *Advances in X-ray Analysis*, Vol. 20 (Denver X-ray Conference, Denver, CO, 1998). JCPDS-International Centre for Diffraction Data, Newtown Square, PA, 2000.

²⁶E. F. Osborn and A. Muan, "Phase Equilibrium Diagrams of Oxide Systems"; Plate 5. American Ceramic Society and the Edward Orton Jr., Ceramic Foundation, Columbus, OH, 1960. E. M. Levin, C. R. Robbins, and H. F. McMurdie, "System $\text{SiO}_2\text{-Al}_2\text{O}_3\text{-K}_2\text{O}$ "; p. 156 in *Phase Diagrams for Ceramists*. 1964. Edited by M. K. Reser. American Ceramic Society, Columbus, OH; Fig. 407.

²⁷C. G. Bergeron and S. H. Risbud, *Introduction to Phase Equilibria in Ceramics*; p. 158. American Ceramic Society, Columbus, OH, 1984.

²⁸W. M. Carty and U. Senapati, "Porcelain—Raw Materials, Processing, Phase Evolution, and Mechanical Behavior," *J. Am. Ceram. Soc.*, **81** [1] 3–20 (1998).

²⁹M. Regueiro and L. Céspedes, "Los yacimientos de materias primas de la Fabrica de Porcelanas del Buen Retiro (1759–1808)" (The Raw Materials Quarries of the Buen Retiro Porcelains Factory) Project 06/0104/99, Las Porcelanas del Buen Retiro, Dirección Gral. de Investigación de la CAM, Madrid, Spain, 2000–2001.

³⁰A. M. Pollard and N. D. Wood, "Development of Chine Porcelain Technology at Jinsgdeshen"; pp. 105–14 in *Proceedings of the 24th International Archaeometry Symposium*. Edited by J. S. Olin and M. J. Blackman. Smithsonian Institution Press, Washington, D.C., 1986.

³¹J. F. Schairer, "The System K_2O – MgO – Al_2O_3 – SiO_2 ; I. Results of Quenching Experiments on Four Joins in the Tetrahedron Cordierite–Forsterite–Leucite–Silica and on the Join Cordierite–Mullite–Potasj Feldspar," *J. Am. Ceram. Soc.*, **37** [11] 501–33 (1954).

³²W. C. Luth, "The System $KAlSiO_4$ – Mg_2SiO_4 – $KAlSi_2O_6$," *J. Am. Ceram. Soc.*, **50** [4] 174–76 (1967).

³³E. N. Maslen, V. A. Streltsov, N. R. Streltsova, N. Ishizawa, and Y. Satow, "Synchrotron X-ray Study of the Electron Density in α - Al_2O_3 ," *Acta Crystallagr., Sect. B: Struct. Sci.*, **39**, 973–80 (1983).

³⁴R. J. Angel, R. K. McMullan, and C. T. Prewitt, "Substructure and Superstructure of Mullite by Neutron Diffraction," *Am. Mineral.*, **76**, 332–42 (1991).

³⁵J. V. Smith, "Crystal Structure of Protoenstatite," *Geol. Soc. Am. Bull.*, **12**, 515–19 (1959).

³⁶G. Will, M. Belloto, W. Parrish, and M. Hart, "Crystal Structure of Quartz and Magnesium Germinate by Profile Analysis of Synchrotron-Radiation High-Resolution Powder Data," *J. Appl. Crystallogr.*, **21** [2] 182–91 (1988).

³⁷D. R. Peacor, "High-Temperature Single-Crystal Study of the Cristobalite Inversion," *Z. Kristallogr., Kristallgeom., Kristallphys., Kristallchem.*, **138**, 274–98 (1973). □